Effect of phase locking on the dynamics of the anti-Stokes component of stimulated Raman scattering

V. S. Butylkin, V. G. Venkin, V. P. Protasov, P. S. Fisher, Yu. G. Khronopulo, and M. F. Shalyaev

Institute of Radio and Electronics, USSR Academy of Sciences
(Submitted August 1, 1975)
Zh. Eksp. Teor. Fiz. **70**, 829–839 (March 1976)

Quantitative measurements were made of the energy characteristics of the axial and conical emission of the anti-Stokes component of stimulated Raman scattering in compressed He_2. A significant difference is observed between the dependences of the energies $W_a^{(ax)}$ and $W_a^{(con)}$ of these components on the pump energy W_p, namely, a nonmonotonic $W_a^{(ax)}(W_p)$ dependence and a monotonic $W_a^{(con)}(W_p)$ dependence. An anomalous decrease of $W_a^{(ax)}$ is observed with decreasing thickness of the material layer. It is shown that this as well as a number of other singularities of the behavior of the anti-Stokes component (whether axial or conical) can be attributed to the limited space in which phase locking of the interacting waves (i.e, nonlinear synchronism) takes place. This limitation on the space is due to the reactions of the Stokes and anti-Stokes components on the pump.

PACS numbers: 42.65.Dr, 67.40.Wt

1. INTRODUCTION

Anti-Stokes stimulated Raman scattering (ASRS) in non-inverted media is the result of parametric interaction of the pump wave and the Stokes component of the SRS. The ASRS was the first experimentally-observed[1] four-wave interaction of light waves, and its theoretical investigation has been the subject of a large number of papers (see, e.g.[2–4]). Nonetheless, numerous experiments have revealed a number of peculiarities of ASRS, which have not been explained by the theory.[5–8]

A. Besides the conical scattering that satisfies the conditions for nonlinear wave synchronism, an axial component was observed, propagating in the direction of the pump beam. In many experiments, this component, for which the wave detuning is appreciable, appears ahead of the conical component.[9] The first explanation of this fact as being due exclusively to the influence of self-focusing[1] was refuted by observation of axial ASRS in gases and liquids, where there was no self-focusing.[8,11]

B. The energy behavior of the anti-Stokes component as a function of the thickness of the scattering layer and of the pump energy differs greatly from the behavior of the Stokes component, although the growth rates for both components, calculated under the assumption of a given pumping, are the same.[2]

C. There is a difference also in the energy behavior of the conical and axial components, as observed by Prokhorov and Sushchinskii.[11] This difference was large enough for them to advance the hypothesis that the axial and conical ASRS are of different origin.

In our brief communication[12] we have shown theoretically and experimentally that the singularities of the axial ASRS can be attributed to effects due to the phase difference of the interacting waves, which is altered by the reaction of the Stokes and anti-Stokes components on the pump. Of decisive significance here is the fact that locking of the generated field phases takes place

over a length greatly exceeding the linear synchronism length (in other words, nonlinear synchronism occurs). The present article is devoted to a detailed exposition of the results of an investigation of both the axial and conical ASRS components, undertaken to explain why these components differ in their behavior from each other and from the Stokes component. We shall see that all the foregoing properties of the ASRS can also be attributed to phase locking of the interacting waves, with allowance for the lengths of their interaction under the concrete experimental conditions.[1)]

2. POLARIZATION AND INITIAL EQUATIONS

Assume that three waves, the pump and its Stokes and anti-Stokes components, propagate in a Raman-active medium (with frequencies ω_p, ω_S, and ω_a, respectively). The resonance conditions for the frequencies of the fields and the medium are

$$\omega_{21} = \omega_p - \omega_S = \omega_a - \omega_p. \tag{1}$$

In the derivation of the equations for the amplitudes and phases of the interacting fields and for the polarization of the medium, we make the following assumptions:

1) Each electromagnetic wave

$$\mathbf{E}_j = \mathbf{e}_j A_j \exp i[\omega_j t - \mathbf{k}_j \mathbf{r} + \varphi_j(r)] + \text{c.c.}$$

is linearly polarized, and all three polarization vectors $\mathbf{e}_j$ ($j = p$, S, a) lie in one plane (these conditions are satisfied in our experiments);

2) The interaction is quasi-stationary, corresponding to the conditions of experiments with lasers operating without mode locking;

3) The nonresonant part of the linear polarization can be neglected (in gasses it is smaller by four or five orders of magnitude than the resonant part[15]).

Under these assumptions, using the procedure described in[16–18], we can obtain expressions for the projections of the components of the polarization on the

field directions:

$$(e_p P_{\omega_p}) = -i\frac{TnN}{\hbar^3}[\bar{r}_S{}^2 A_S{}^2 - \bar{r}_a{}^2 A_a{}^2]A_p \exp i(\varphi_p - k_p r),$$

$$(e_S P_{\omega_S}) = i\frac{TnN}{\hbar^3}[\bar{r}_S{}^2 A_S + \overline{r_S r_a} A_a e^{-i\theta}]A_p{}^2 \exp i(\varphi_S - k_S r), \qquad (2)$$

$$(e_a P_{\omega_a}) = -i\frac{TnN}{\hbar^3}[\bar{r}_a{}^2 A_a + \overline{r_S r_a} A_S e^{-i\theta}]A_p{}^2 \exp i(\varphi_a - k_a r).$$

Here $\theta = \varphi_S + \varphi_a - 2\varphi_p + (\Delta \cdot r)$; $\Delta = 2k_p - k_S - k_a$; N is the number of molecules per cubic centimeter; T is the reciprocal half-width of the resonant-transition line

$$r_S = \sum_k \left(\frac{(d_{ki} e_S)(d_{2k} e_p)}{\omega_{k2} + \omega_p} + \frac{(d_{ki} e_p)(d_{2k} e_S)}{\omega_{k2} - \omega_S} \right);$$

r_a is obtained from r_S by the subscript interchange $S \to p$ and $p \to a$; a bar over r_a or r_S denotes averaging over the molecule orientation. The time variation of the difference n between the populations of the levels 1 and 2 is described by the equations[2]

$$\frac{dn}{dt} = \frac{n_0 - n}{\tau} - 4\frac{Tn}{\hbar^3}(\bar{r}_S{}^2 A_S{}^2 + \bar{r}_a{}^2 A_a{}^2 + 2\overline{r_S r_a} A_S A_a \cos\theta) A_p{}^2,$$

where τ is the lifetime in the excited state, and n_0 is the equilibrium difference of the populations in the absence of fields.

We shall henceforth neglect the population saturation, inasmuch as $n \approx n_0$ in experiments with pulse duration $\sim 10^{-8}$ sec and intensity less than 10 GW. The wave equation for the field component at the frequency ω_j in an isotropic weakly-nonlinear medium can be written in the form[19]

$$-A_j(k_j \operatorname{grad} \varphi_j) + i(k_j \operatorname{grad} A_j) = \frac{2\pi\omega_j^2}{c^2}(e_j P_{\omega_j}). \qquad (3)$$

Using (2) and (3), we write down a system of equations for the dimensionless real amplitudes of the fields and for the phase difference

$$\frac{\partial a_p}{\partial \xi} = (r_1 a_a{}^2 - a_S{}^2) a_p \cos(\alpha_p - \alpha_a), \qquad (4a)$$

$$\frac{\partial a_S}{\partial \xi} = q_S(a_S + r_2 a_a \cos\theta) a_p{}^2 \cos(\alpha_S - \alpha_a), \qquad (4b)$$

$$\frac{\partial a_a}{\partial \xi} = -q_a(r_1 a_a + r_2 a_S \cos\theta) a_p{}^2, \qquad (4c)$$

$$\frac{\partial\theta}{\partial\xi} = r_2\left[q_a\frac{a_S}{a_a} - q_S\frac{a_a}{a_S}\cos(\alpha_S - \alpha_a)\right] a_p{}^2 \sin\theta + \delta. \qquad (4d)$$

Here $a_j = A_j/A_{p0}$ (where $A_{p0} = A_p|_{z=0}$); $\alpha_{p,S,a}$ are the angles between $k_{p,S,a}$ and the z axis;

$$\xi = z\frac{2\pi\omega_p^2 TnN\bar{r}_S^2}{\hbar^3 c^2 k_p \cos\alpha_a}A_{p0}{}^2, \qquad \delta = \Delta_a \bigg/ \frac{2\pi\omega_p^2 TnN}{\hbar^3 c^2 k_p}\bar{r}_S^2 A_{p0}{}^2,$$

where Δ_a is the projection of Δ on k_a;

$$q_{S,a} = \omega_{S,a}^2 k_p / \omega_p^2 k_{S,a}; \quad r_1 = \overline{r_a^2}/\bar{r}_S^2; \quad r_2 = \overline{r_S r_a}/\bar{r}_S^2.$$

We note that Eqs. (4) describe both the conical and the axial components of the ASRS; the difference lies only in Δ_a and in the angles α_p, α_S, and α_a. The main parameter whose variation leads to qualitative differences in the behaviors of these components is the quantity δ.

3. SPATIAL DISTRIBUTION OF THE ANTI-STOKES COMPONENT

The solution of Eqs. (4) for a given pump field (a_p = const) was investigated in detail in Bloembergen's book.[2] His approach, however, does not correspond to the conditions of experiments in which an appreciable energy transfer takes place at least to one of the scattering components—the Stokes component. Let us obtain the solution of (4) with allowance for the influence of this component on the pump under the condition that the detuning δ is large enough and the power of the anti-Stokes component is low, so that its reaction on the pump can be neglected. The behavior of the pump and of the Stokes component of the SRS is described approximately by the solution of the first two equations of (4), in which $a_a = 0$[20]

$$a_p{}^2 = a_{p0}\frac{1+M}{1+Me^{\varkappa\xi}}, \qquad a_S{}^2 = a_{S0}\frac{(1+M)e^{\varkappa\xi}}{1+Me^{\varkappa\xi}},$$

where

$$M = a_{S0}{}^2/q_S a_{p0}{}^2, \quad \varkappa = 2q_S a_{p0}{}^2(1+M),$$
$$a_{p0} = a_p|_{z=0}, \quad a_{S0} = a_S|_{z=0}.$$

Substituting this into the equation for the complex amplitude $(a_a \exp[i\varphi_a])$, we obtain

$$\frac{\partial(a_a e^{-i\varphi_a})}{\partial\xi} = -q_a a_p{}^2\{r_1(a_a e^{-i\varphi_a}) + r_2 a_S e^{i\delta\xi}\}.$$

Solving the obtained expression, we find that the behavior of the amplitude of the anti-Stokes component is described by the Gauss hypergeometric function $_2F_1$:

$$a_a e^{-i\varphi_a} = a_{S0}R\,\frac{r_2}{r_1}\frac{(1+M)^{-(R+i\tilde\delta)}}{(1-i\tilde\delta)}\frac{(M+e^{\varkappa\xi})^R}{M^{R+R+i\tilde\delta}}\left\{\left(\frac{1+M}{1+Me^{\varkappa\xi}}\right)^{1-i\tilde\delta}{}_2F_1\left(\frac{1}{2}-R\right.\right.$$

$$\left.\left. -i\tilde\delta, 1-i\tilde\delta; 2-i\tilde\delta; \frac{1}{1+Me^{\varkappa\xi}}\right) - {}_2F_1\left(\frac{1}{2}-R-i\tilde\delta, 1-i\tilde\delta; 2-i\tilde\delta; \frac{1}{1+M}\right)\right\}, \qquad (5)$$

where

$$\tilde\delta = \frac{\delta}{2(1+M)}, \qquad R = \frac{q_a}{2q_S}r_1.$$

It follows therefore that at distances in which an appreciable part of the pump energy goes over into the Stokes component $a_a(\xi)$ is a nonmonotonic function (see, e.g., the $\delta = -3$ curve on Fig. 1). The reaction of the Stokes component on the pump greatly influences the behavior of the anti-Stokes component of the SRS; ultimately it leads to a loss of the phase locking

$$\lim_{z\to\infty}\theta = (\Delta r).$$

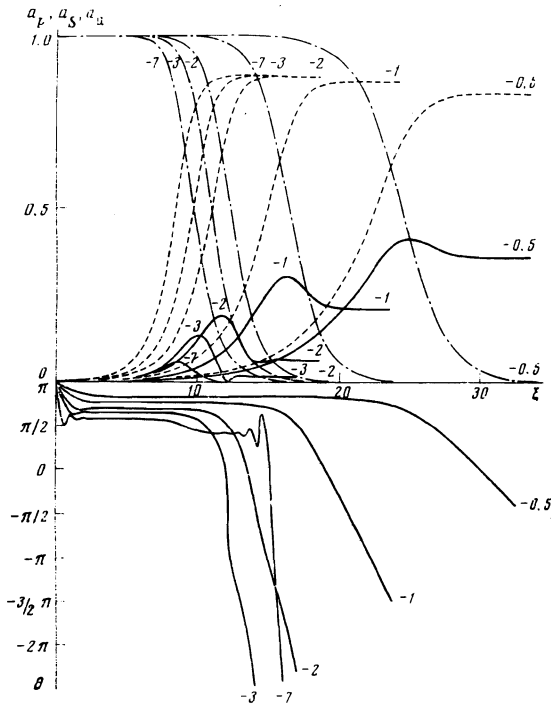As a result, a constant intensity of the anti-Stokes com-

FIG. 1. Plots of a_a (solid curve), a_p (dash-dot), and a_S (dashed), and θ against ξ at $\delta = -7$, -3, -2, -1, and -0.5, obtained for the ratio $\omega_{21}/\omega_p = 0.22$ and for the initial values $a_a|_{\xi=0} = 10^{-6}$, $a_S|_{\xi=0} = 10^{-3}$, $a_p|_{\xi=0} = 1$, and $\theta|_{\xi=0} = \pi$. It is assumed that $r_1 = r_2 = 1$.

ponent is established:

$$\lim_{z \to \infty} a_a^2 = a_{p0}^2 \frac{q_a^2 r_2^2}{q_S(1+2R)^2} \frac{\pi\delta/2}{\text{sh}(\pi\delta/2)} \prod_{m=0}^{\infty}\left\{1 + \frac{\delta^2}{(1+2R+2m)^2}\right\}^{-1} = \text{const.}$$

(6)

In expression we have neglected the ratio of the number of photons of the Stokes component and of the pump at the input in comparison with unity ($M \ll 1$).

With increasing input pump energy, the limiting value of the amplitude (6) becomes comparable with the amplitudes of the pump and of the Stokes component, so that solution (5) cannot be used if

$$\frac{\pi}{2}\delta < 1, \quad \text{i.e., at} \quad A_{p0}^2 > \frac{\hbar^3 c^2 k_p \Delta_a}{4\omega_p^2 T n N \bar{r}_S^2}.$$

To describe the behavior of the anti-Stokes component in this case it is necessary to take into account its reaction on the pump and on the Stokes component. It is impossible to obtain an analytic solution of the system (4). It is easy to see from (4), however, that the qualitative picture of the behavior of $a_a(\xi)$ remains the same also for large pumps (small δ). Indeed, it is seen from (4d) that at the start of the interaction, inasmuch as $a_S a_p^2/a_a \gg 1$, the phase difference is

$$\theta \approx \pi + \arcsin\left[\delta \left/ r_2\left(q_a\frac{a_S}{a_a} - q_S\frac{a_a}{a_S}\right)a_p^2\right.\right]$$

(7)

(at large pumps we have $\theta \approx \pi$). The anti-Stokes component increases, since the parametric energy transfer

from the Stokes wave and from the pump into the anti-Stokes wave ($a_S + a_p \to a_a$; see the second term of (4c)) exceeds the pure Raman conversion of the anti-Stokes component into the pump ($a_a \to a_p$). Further, as a result of the decrease of a_p, the phase decreases in such a way that the rate of growth of a_a decreases. This accelerates the conversion $a_p \to a_S$ and leads to an even faster deviation of the phase from π. When θ deviates from π to such an extent that the processes $a_S + a_p \to a_a$ and $a_a \to a_p$ are balanced, a_a reaches a maximum and then decreases. Since a_S continues to increase, the pump ultimately decreases to a very low value and the wave interaction practically ceases; a constant value of a_a is established and $\theta \approx (\Delta \cdot \mathbf{r})$.

A computer solution of Eqs. (4) confirms the described qualitative picture. Figure 1 shows plots of $a_a(\xi)$ for different values of Δ_a at a constant pump I_{p0}.[3]

We note one consequence of the plots of Fig. 1. From calculations of the growth rate of the anti-Stokes wave in the given-pump approximation it follows that at a certain $\delta = \delta_m$ the initial growth of $a_a(\xi)$ is maximal. It is seen from Fig. 1, however, that as $|\delta|$ decreases (that is, as the pump increases or as the detuning $|\Delta_a|$ decreases) the value of $\lim_{z \to \infty} a_a$ increases. Therefore, for a fixed interaction length L, the pump at which the power of the anti-Stokes component is maximal can correspond to a value $|\delta| < |\delta_m|$.

4. ENERGY CHARACTERISTICS OF ASRS

With the aid of the solution for a_a (Fig. 1) we can find the dependence of the output energy of the anti-Stokes component on the input pump energy for a fixed wave-interaction length L. It is obvious that this dependence is nonmonotonic (see Fig. 2). First, with increasing I_{p0}, a burst of intensity of the anti-Stokes component I_a appears and is due to the passage of the maximum of the corresponding $a_a(\xi, \delta)$ curve through the exit from the chamber ($z = L$) (see Fig. 1). Then $I_a(I_{p0})|_{z=L}$ again begins to grow. Ultimately the output intensity I_a will again decrease with increasing I_{p0}, inasmuch as at $|\delta| < |\delta_m|$ the rate of growth of $a_a(\xi)$ decreases; the rate of growth of the Stokes component also decreases. The last fact can explain, in particular, the experimentally observed asymmetry of the energies of the Stokes SRS components propagating in the forward and backward directions in the case of strong pumping[21] (for example, when the pump is focused into the working medium). For backward waves we have $|\Delta| \sim |k|$, as a result of which phase locking is not feasible at realistic powers I_{p0} and no anti-Stokes wave is produced.

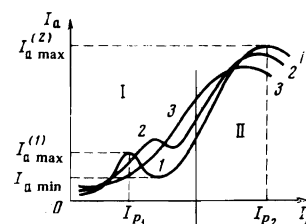
FIG. 2. Plots of $I_a(I_{p0})$. 1) $\Delta_a = \Delta_1$; 2) $\Delta_a = \Delta_2$; 3) $\Delta_a = \Delta_3$. $|\Delta_1| > |\Delta_2| > |\Delta_3|$.

We consider now the difference between the plots of $I_a(I_{p0})$ for the axial and conical ASRS. We note that calculation of the angular distribution requires in the general case a simultaneous solution of the equations for the interacting waves with allowance for the spatial spectrum of the Stokes and anti-Stokes components, an exceedingly complicated problem even for a numerical computer analysis. At pump energies, however, at which a clear-cut separation of the axial and the conical ASRS is ensured, certain qualitative behavior features that distinguish the conical component from the axial one can be established. We use for this purpose the results of the calculation of the function $I_a(I_{p0})$ for different values of Δ_a, shown in Fig. 2.

In region II, the faster saturation and the subsequent decrease of the intensity of the conical ASRS in comparison with the axial one is due to the fact that the dimensionless detuning $\delta = \delta_m$ for this component is reached at lower pumps. In the initial section (in region I), however, the first maximum of I_a shifts into the region of large pumps with decreasing Δ_a; the "dip" on the section of the $I_a(I_{p0})$ curve then decreases and practically vanishes for the component propagating in the direction for which $|\delta| < |\delta_m|$. It is this fact which determines the qualitative differences in the behavior of $I_a(I_{p0})$ for the conical and axial ASRS.

These properties of the ASRS are due to the following causes: Nonmonotonicity of $I_a(I_{p0})$ in region I (Fig. 2) can be observed when the loss of the phase locking occurs at $z < L$ (see the plot of $a_a(\xi)$ in Fig. 1). With decreasing $|\Delta_a|$, the loss of the phase locking over the interaction length occurs at I_{p0} larger than for the axial direction.

As a result, the decrease of I_a after passing through $I_{a\,max}^{(1)}$ will also be small, since the difference between the maximum and asymptotic values of the $a_a(\xi)$ curves decreases with decreasing Δ_a.

Thus, the nonmonotonic behavior of I_a on the initial section is most strongly pronounced for the axial component of the ASRS.

Similar reasoning in the case of a given value of the detuning Δ_a shows that the value of $I_{a\,max}^{(1)}$ decreases with increasing interaction length L (see Fig. 2 of[12]). At the same time, at sufficiently small L the difference between $I_{a\,max}^{(1)}$ and $I_{a\,min}^{(1)}$ decreases. As a result there should exist a length L that is optimal for the observation of the nonmonotonicity of $I_a(I_{p0})$.

Thus, we can formulate the following qualitative features of the behavior of the axial and conical components of the ASRS: a) the behavior of the intensity of the axial anti-Stokes component with increasing pump is nonmonotonic; b) as the direction of exact synchronism is approached, the nonmonotonicity of $I_a(I_{p0})$ becomes less and less pronounced; c) an increase of the interaction length should lead to a decrease of the maximum $I_{a\,max}^{(1)}$ and to its shift to weaker pumps; d) the intensity $I_a(L)$ at the output (after passing through $I_{a\,min}^{(1)}$) does not depend on the length L at constant Δ_a and at sufficiently strong pumping; e) the intensity of the

Stokes component $I_S(I_{p0})$ changes monotonically at all values of Δ_a.

All the foregoing results were obtained from Eqs. (4), which describe the interaction of plane waves. It must be recognized that under real conditions, even in a plane pump wave, a complicated angular distribution of the scattering components occurs.[22] The situation becomes even more complicated if it is recognized that the transverse section of the pump beam is bounded and its pulse is not rectangular in time or space. All this makes it difficult to observe the above-mentioned singularities. Thus, if one measures the integrated energy W_a of the anti-Stokes component, then the deviation from rectangularity of the space-time distribution of the pump leads to a smoothing of the $W_a(W_{p0})$ dependence in comparison with the intensity dependence shown in Fig. 2. A computer calculation shows that at a Gaussian pump-beam cross section and a Gaussian temporal distribution the dips on the $W_a(W_{p0})$ can give way to "plateaus" whose heights decrease with increasing L.

Further, with increasing pump the intensity of the Stokes component of scattering to the pump-beam axis increases. As result of the phase locking, the contribution to the intensity I_a in a certain fixed direction gives an ever-increasing number of waves with different values of Δ_a, and this leads to a "smearing" of the angular spectrum of the ASRS.

5. EXPERIMENTAL PART

The main purpose of the experiment was to observe the ASRS singularities noted above. As the Raman-active medium we used hydrogen. The pump was the second harmonic of a one-mode neodymium-glass laser (the experimental setup is shown in Fig. 3). Pump radiation of duration $\sim 3 \cdot 10^{-8}$ sec and energy up to 0.3 J had a nearly Gaussian intensity distribution over the beam cross section.

Experiments were performed with different lengths of chambers, hydrogen pressures, and different focal lengths of the lens L_1. Characteristic plots of the dependence of the energies of the axial, conical, and in-
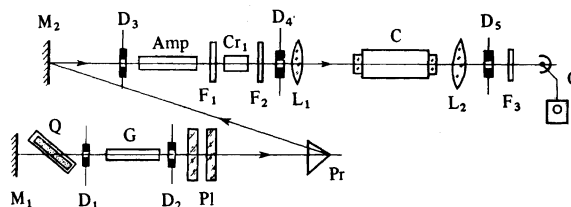

FIG. 3. Experimental setup. C—chamber with compressed hydrogen; G—active element of driving generator—neodymium glass 10 mm diameter × 130 mm; M_1, M_2—mirrors reflecting 100% of the radiation of wavelength 1.06 μ; Pl—plane-parallel glass plates, which form together with mirror M_1 the resonator of the master generator; Q—passive Q-switch—solution of dye No. 3955 in dimethyl sulfoxide; Pr—rotating prism; D_1–D_5—diaphragms; Amp—4-stage amplifier for the radiation of the single-mode driving generator. F_1–F_3—light filters; Cr_1—KDP frequency-doubling crystals; L_1, L_2—lenses, O—photoreceiver and oscilloscope with memory.
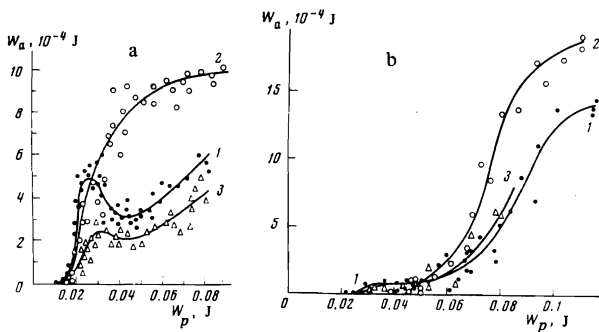
FIG. 4. Dependence of the energy of the axial (1), conical (2), and intermediate (3) ASRS components on the pump energy. Hydrogen pressure 75 atm. The focal length of lens L_2 is 50 cm. Diaphragm D_5 at the focus of the lens L_2—round aperture, 2 mm-diameter (curve 1); round shutter, 6 mm diameter (curve 2); annular opening with inside diameter 3 mm and outside diameter 6 mm (curve 3). Focal length of the lens L_1—100 cm (4a) and 200 cm (4b). Length of chamber C—13 cm (4a) and 6.5 cm (4b).

FIG. 6. Angular distribution of the anti-Stokes SRS component at three values of the pump energy: a) 0.028 J; b) 0.049 J; c) 0.11 J. Hydrogen pressure 80 atm; length of chamber C—13 cm; focal length of lens L_1—200 cm; of lens L_2—50 cm. The photographic film was placed at the focus of lens L_2. The diameter of the "ring" of the conical component of the ASRS is $\approx$ 8 mm under these conditions (Fig. 6b).

termediate parts of the ASRS on the pump energy as shown in Fig. 4. It is seen that the behavior of the axial and conical components agrees qualitatively with the theoretical predictions. The conical component increases monotonically and is saturated before the axial component. The pump intensity at which this saturation is noticeable ($\sim$ 3.0 GW/cm^2) agrees in order of magnitude with the calculated one (Fig. 2).

A dip is clearly seen on the plot of the axial part of the ASRS (Fig. 4a). The pump intensity at which the axial component has an intensity extremum is 1.5–2.0 GW/cm^2 and is close to the calculated value. We note that the results shown in Fig. 4a of the present paper and in Fig. 3 of our earlier paper[12] agree, in spite of some differences in the experimental conditions. The maxima in both cases are observed at close values of the pump intensities. In[12] the chamber length (5 cm) was significantly smaller than the length of the focal region; in the present study the length of the focal region produced by the lens L_1 was 4 cm and was smaller than the chamber length (13 cm). The agreement of the results for these two cases indicates that the interaction region can be identified quite accurately with the length of the focal region.

Let us discuss briefly the behavior of the anti-Stokes component energy in the region between the axis and
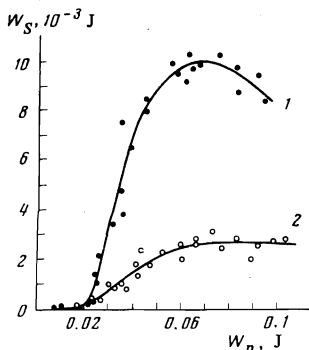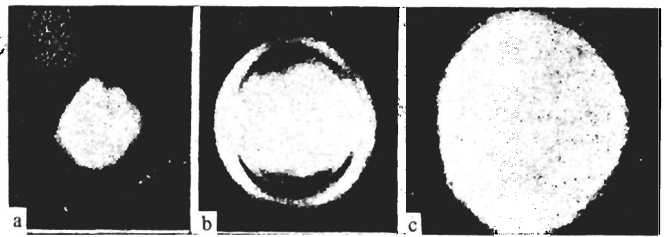

FIG. 5. Dependence of the SRS Stokes-component energy on the pump energy. 1) "Axial" part of the SRS Stokes component, corresponding to curve 1 of Fig. 4a. 2) "Conical" part of the Stokes component of the SRS corresponding to curve 2 of Fig. 4a.

the synchronism cone (curve 3 of Fig. 4). The ASRS intensity in this region (in the pump range used in the present experiment) is much lower than the intensity of the axial and conical components. Curve 3 of Fig. 4a is similar to curve 1, but the dip on it is less pronounced. This can be explained by making the natural assumption that the main contribution to the ASRS intensity in this region is made by plane waves with a wave mismatch $|\Delta_a|$ larger than for the conical ASRS, but smaller than for the axial one (see Fig. 2).

Figure 4b shows results obtained for a focal region of 12-cm length (see also Fig. 3 of[12]). In accord with the results of the preceding section, the energy of the anti-Stokes component turned out to be smaller for the larger interaction length.

We investigated also the pump dependence of the intensity of the SRS Stokes component emitted into the same solid angles in which the ASRS was investigated. The results obtained under the same conditions as the curves of Fig. 4a are shown in Fig. 5. Both the axial and conical Stokes components increase monotonically in the range of variation of the pump energy from 0.01 to 0.06 J, in which curve 1 of Fig. 4a has a dip. The saturation and the decrease of the intensity of the axial Stokes component are due to the onset of a second-order Stokes component at pump energies exceeding 0.07 J, that is, beyond the limits of the pump-energy interval in which the characteristic singularities in the behavior of the axial ASRS component were observed.

Figure 6 shows a photograph of the angular distribution of the ASRS, obtained at a pump beam diameter in the chamber 0.08 cm. It is seen that the threshold is reached earlier than for the axial ASRS, and a conical component appears; with further increase of the pump, all the directions inside the cone corresponding to the synchronism angle become filled.

At a pump beam of 0.3-mm diameter, the conical ASRS is primarily produced. Thus, the differences in the ratio of the thresholds of the axial and conical ASRS can be attributed to the dependence of these thresholds on the pump-beam diameter. The increase of the latter increases the interaction length for the conical SRS component, and this lowers the value of the pump at which the conical ASRS reaches a value that can be registered.

We note that no focusing effects were observed in our experiments; moreover, estimates of the focal length of the lens formed by the SRS conversion[23] show that even for the longest of the chambers employed by us the increase of the power density in the beam can be neglected. Other causes of self-action, such as the optical Kerr effect, electrostriction, and thermal self-focusing are known to be even less significant for hydrogen.

6. CONCLUSION

ASRS, as all other four-wave interactions that can occur effectively in the absence of linear synchronism conditions, are referred to in the literature as belonging to "class II."[9,10,21] We have shown here that all the regularities of the behavior of the ASRS, including the axial one, are due to phase locking and to the limit length over which this phenomenon takes place. The phase-locking length in ASRS is determined by the characteristic length of the conversion of the pump wave into the Stokes component; this length is usually much larger than the linear-synchronism length, and this ensures the possibility of an intense growth of the anti-Stokes component. It can be assumed that the phase locking is the same phenomenon which (with allowance for the limitation on the space in which the phase locking takes place) explains all the singularities of "class II" scattering.

1) Phase locking of interacting fields is well known from radio engineering.[13] The possibility of its realization in nonlinear optics was first demonstrated by Akhmanov and co-workers[14] using as an example the subharmonic generation in a nonresonant dissipative medium. Phase locking in ASRS was not discussed prior to our paper,[12] although it is contained explicitly in the solutions obtained in the given-pump approximation.[2-4] These solutions do not describe the loss of phase stability, for which allowance must be made for a correct explanation of the ASRS behavior.

2) It is assumed that n is the same for all sublevels of states 1 and 2 with different angular momenta.

3) See also Fig. 1 of[12], which shows the behavior of $a_{a,s,p}(z)$ at constant Δ_a and different values of the pump I_{p0}.

[1] R. W. Terhune, Bull. Am. Phys. Soc. 2, 8, 359 (1963).

[2] N. Bloembergen, Nonlinear Optics, Benjamin, 1965 (Russ. Transl., Mir, 1966).

[3] V. N. Lugovoǐ and I. I. Sobel'man, Zh. Eksp. Teor. Fiz. 58, 1283 (1970) [Sov. Phys. JETP 31, 690 (1970)].

[4] V. N. Lugovoi, Vvedenie v teoriyu vynuzhdennogo kombinatsionnogo rasseyaniya (Introduction to the Theory of Stimulated Raman Scattering), Nauka, 1968.

[5] E. Garmire, An Investigation of Stimulated Raman Emission, Ph. D. dissertation, MIT, 1965.

[6] R. W. Minck, R. W. Terhune, and W. G. Rado, Appl. Phys. Lett. 3, 181 (1963).

[7] A. I. Sokolovskaya, A. D. Kudryavtseva, and M. A. Sushchinskiǐ, Trudy 2-go Vsesoyuznogo simpoziuma po nelinneǐnoǐ optike (Proc. 2nd All-Union Symposium on Nonlinear Optics), Novosibirsk, 1966, Nauka, 1968, p. 277.

[8] G. V. Venkin, Candidate's dissertation, Moscow State Univ., 1971.

[9] A. I. Sokolovskaya, E. A. Morozova, A. D. Kudryavtseva, and M. M. Sushchinskiǐ, Kvantovaya Elektron. (Moscow) No. 4 (16), 76 (1973) [Sov. J. Quantum Electron. 3, 321 (1973)].

[10] K. Shimoda, Jap. J. Appl. Phys. 5, 86 (1966).

[11] K. A. Prokhorov and M. M. Sushchinskiǐ, Kratk. Soobshch. Fiz. 5, 48 (1970).

[12] V. S. Butylkin, G. V. Venkin, V. P. Protasov, N. D. Smirnov, Yu. G. Khronopulo, and M. F. Shalyaev, Pis'ma Zh. Eksp. Teor. Fiz. 17, 400 (1973) [JETP Lett. 17, 285 (1973)].

[13] I. M. Kapchinskiǐ, Metody teorii kolebaniǐ v radiotekhnike (Methods of Oscillation Theory in Radio), Gosenergoizdat, 1954.

[14] S. A. Akhmanov, V. G. Dmitriev, V. P. Modenov, and V. V. Fadeev, Radiotekh. Élektron. 10, 2157 (1965).

[15] W. G. Rado, Appl. Phys. Lett. 11, 123 (1967).

[16] Yu. G. Khronopulo, Izv. Vyssh. Uchebn. Zaved. Radiofiz. 7, 674 (1964).

[17] V. S. Butylkin, G. L. Gurevich, M. I. Kheifets, Yu. G. Khronopulo, Izv. Vyssh. Uchebn. Zaved. Radiofiz. 9, 545 (1966).

[18] G. L. Gurevich and Yu. G. Khronopulo, Zh. Eksp. Teor. Fiz. 51, 1499 (1966) [Sov. Phys. JETP 24, 1012 (1967)].

[19] S. A. Akhmanov and A. S. Chirkin, Statisticheskie yavleniya v nelineǐnoǐ optike (Statistical Phenomena in Nonlinear Optics), MGU, 1971.

[20] V. T. Platonenko and R. V. Khokhlov, Zh. Eksp. Teor. Fiz. 46, 555 (1964) [Sov. Phys. JETP 19, 378 (1964)].

[21] A. D. Kudryavtseva, A. I. Sokolovskaya, and M. M. Sushchinskiǐ, Zh. Eksp. Teor. Fiz. 59, 1556 (1970) [Sov. Phys. JETP 32, 849 (1971)].

[22] D. N. Klyshko, Zh. Eksp. Teor. Fiz. 64, 1160 (1973) [Sov. Phys. JETP 37, 590 (1973)].

[23] V. P. Protasov, Kandidatskaya dissertatsiya, MGU, Candidate's Dissertation, Moscow State Univ., 1974.

Translated by J. G. Adashko